Linear Dichroism in Resonant Inelastic X-Ray Scattering to Molecular Spin-Orbit States

R. Guillemin,[1,2] S. Carniato,[1,2] W. C. Stolte,[3,4] L. Journel,[1,2] R. Taïeb,[1,2] D. W. Lindle,[3] and M. Simon[1,2]

[1]*UPMC Univ Paris 06, UMR 7614, Laboratoire de Chimie Physique Matière et Rayonnement, F-75005 Paris, France*
[2]*CNRS, UMR 7614, Laboratoire de Chimie Physique Matière et Rayonnement, F-75005 Paris, France*
[3]*Department of Chemistry, University of Nevada, Las Vegas, Nevada 89154-4003, USA*
[4]*Advanced Light Source, Lawrence Berkeley National Laboratory, Berkeley, California 94720, USA*

(Received 28 March 2008; published 25 September 2008)

Polarization-dependent resonant inelastic x-ray scattering (RIXS) is shown to be a new probe of molecular-field effects on the electronic structure of isolated molecules. A combined experimental and theoretical analysis explains the linear dichroism observed in Cl $2p$ RIXS following Cl $1s$ excitation in HCl and CF_3Cl as due to molecular-field effects, including singlet-triplet exchange, indicating polarized-RIXS provides a direct probe of spin-orbit-state populations applicable to any molecule.

DOI: 10.1103/PhysRevLett.101.133003 PACS numbers: 33.80.Eh, 33.70.Ca, 34.50.Gb

Spin-orbit (SO) interactions most commonly manifest themselves in atomic and molecular spectroscopy as energy splittings among states with the same overall electronic configuration. In atoms, these splittings are well characterized, and spectroscopic intensities generally obey simple statistical rules. For example, atomic core-level photoionization from $2p$ inner shells yields two SO components, $2p_{3/2}$ and $2p_{1/2}$, with a statistical intensity ratio of precisely two. In molecules, core levels are often considered atomiclike, despite the presence of molecular-field (MF) effects inherent to the chemical environment of the elemental component being probed. These MF effects are known to shift core-level (and valence) ionization energies and to induce other subtle changes in molecular spectra. Yet, the tendency to assume molecular inner shells are effectively atomiclike persists because MF effects often appear to induce only minor perturbations on core-level spectra. For instance, moderate-resolution core-level photoemission spectra of molecular $2p$ inner shells show, as for atoms, two peaks with an intensity ratio of about 2:1. Similar results are obtained in molecular x-ray emission when a $1s$ electron is ionized and a KL ($K\alpha$) x ray is emitted as a $2p$ electron fills the K hole. With such techniques, one can observe molecular character in the spectra, such as the aforementioned MF effects, only upon closer inspection.

Recently, high-resolution core-level-photoemission measurements ($\Delta E \sim 40$ meV) identified contributions from three SO sublevels, $^2\Pi_{1/2}$, $^2\Sigma_{3/2}$, and $^2\Pi_{3/2}$, in L-edge photoionization of HCl, arising from coupling between MF and SO interactions in the ionized molecule [1,2]. Other examples also have shown high-resolution photoelectron spectra [3], as well as spin-resolved photoemission [4], can be sensitive probes of molecular environments in ionized species. However, for core-excited neutral states, explored in this work, the situation is more complex. In addition to the MF effects seen in ions, these states also are influenced by singlet-triplet exchange (STE), which contributes to lifting the degeneracy of the $2l + 1$ components of the subshell [5], inducing fluctuations in the SO branching ratios. For excitations to neutral dissociative states, linewidths are broadened by large Franck-Condon envelopes, and direct experimental evidence of fine-structure splittings due to STE is nearly impossible to obtain in x-ray absorption; to garner information on chemical environment while measuring the inner-shell population of SO components, quenching of the Franck-Condon broadening is necessary. In this respect, resonant inelastic x-ray scattering (RIXS) provides a unique approach.

In isolated atoms and molecules, RIXS in the 2–10 keV range has recently experienced growing interest [6–8]. As noted previously [6,9], RIXS measurements in this range take advantage of ultrafast nuclear dynamics and high-energy-resolution decay spectra, taken with long-pulse light sources, using the concept of effective duration time of the scattering process [10,11]. Indeed, dynamical broadening caused by the Franck-Condon distribution is quenched on top of neutral resonances, and widths of x-ray-emission lines approach the core-hole lifetime (Γ_c). This line narrowing is most relevant for transitions occurring between inner shells, such as $2p$ and $1s$, with nearly parallel potential-energy surfaces [6].

In this Letter, we report a combined experimental and theoretical approach using polarized RIXS to probe chemical environments and MF effects. Linear dichroism exhibited in polarized x-ray-emission spectra (see Fig. 1) is shown to be sensitive to coupling between the MF and SO interactions. This result should be completely general, observable in a wide variety of molecular systems. Here, we focus on KL RIXS in two chlorine-containing molecules, HCl and CF_3Cl, in which the chlorine atoms have different chemical environments. Specifically, we consider excitation of an electron from the Cl $1s$ core orbital to the first antibonding molecular orbital ($6\sigma^*$ for HCl, $11a_1^*$ for CF_3Cl). Using measurements at various angles between the polarizations of the incident and scattered photons,

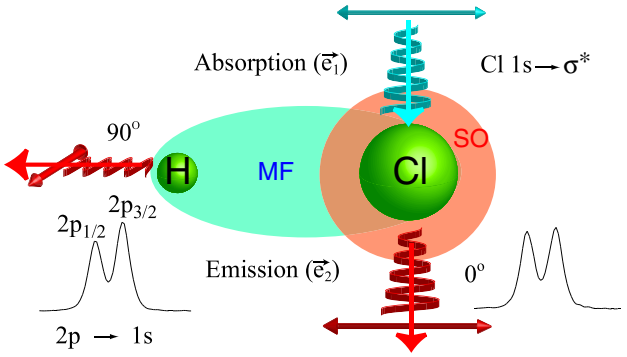

FIG. 1 (color online). Schematic representation of linear dichroism observed in KL x-ray emission from HCl. After resonant K-shell excitation, KL radiative decay is measured at different angles θ between the incident ($\vec{e}_1$) and emitted ($\vec{e}_2$) polarization vectors. Coupling between the spin-orbit interaction and the molecular field, oriented along the chlorine bond, leads to different $2p_{3/2}$:$2p_{1/2}$ spin-orbit ratios as a function of θ.

coupled with *ab initio* calculations, we obtain sensitive determinations of molecular $2p_z$ and $2p_{xy}$ populations in the SO doublets.

Measurements were done at beam line 9.3.1 [12] at the Advanced Light Source in Berkeley CA, which provides intense (10^{11} photons/ sec), monochromatic (0.4 eV at the Cl K edge), and over 99% linearly polarized photons uses a double Si(111) monochromator. X-ray-emission spectra were acquired using a curved-crystal spectrometer [13] consisting of a variable-radius Si(111) crystal and a 2D position-sensitive microchannel-plate resistive-anode detector. A gas cell maintained samples at a static pressure of 400 Torr. At 2620 eV, for the Cl KL spectra, the Bragg reflection condition for Si(111) is fulfilled for 49°, close to the x-ray Brewster angle of 45°. Consequently, contributions from x-rays polarized perpendicular to the surface of the crystal are strongly quenched. By rotating the spectrometer with respect to the incident polarization $\vec{e}_1$, we can analyze the polarization $\vec{e}_2$ of the emitted x rays. Spectra were obtained at 10 different angles with respect to the incident polarization. In this mode, the spectrometer acts both as a polarizer and an energy analyzer because the detector collects a 20-eV-wide KL emission spectrum with 0.5 eV resolution. Spectra of core-excited neutral molecules were collected for HCl on the $1s \rightarrow 6\sigma^*$ resonance and for CF_3Cl on the $1s \rightarrow 11a_1^*$ resonance ($h\nu \sim$ 2823.5 eV in both cases).

Figure 2 shows Cl $2p_{3/2}$:$2p_{1/2}$ SO ratios (open circles) measured on-resonance for HCl and CF_3Cl at various polarization angles of the emitted photons relative to the incident x-ray polarization. The experimental ratios were obtained by treating the spectra (see Fig. 1 for examples) as atomiclike, i.e., simply fitting them to two Voigt profiles. For both molecules, the values differ *significantly* from the statistical atomic $2p$ ratio (2:1). In addition, a clear polarization dependence is observed, with parallel polarization

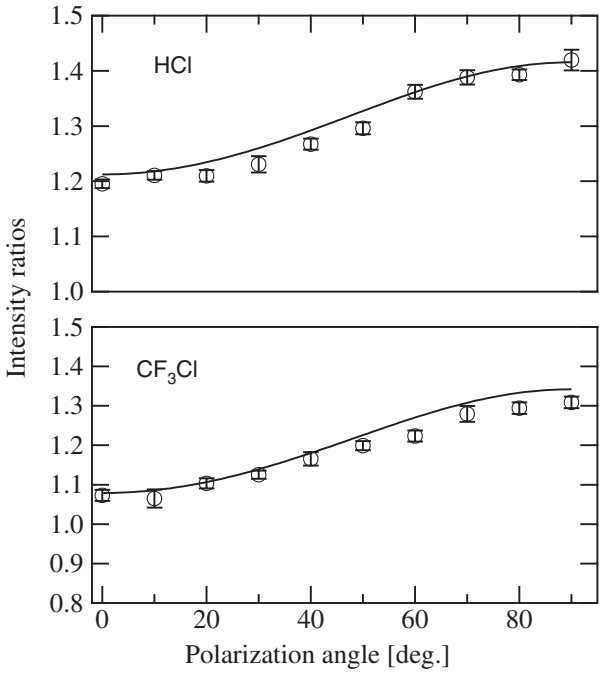

FIG. 2. Experimental and calculated (curves) intensity ratios of spin-orbit components, $2p_{3/2}/2p_{1/2}$, as a function of angle between the polarization vectors of incident and scattered photons. Experimental ratios (circles) were obtained by fitting the spectra with only two SO components (see text for details).

(0°) showing the largest deviation from the statistical ratio in each case. The spectra also exhibit subtle changes in the apparent SO splitting as a function of polarization angle. Together, these two key experimental findings suggest the presence of additional structure within the (nominally) two-peak KL-emission spectra.

Although gases are randomly oriented, anisotropy of polarized x-ray emission from core-excited molecules is well established [14,15]. Because dipole selection rules impose symmetry restrictions in both absorption and emission [16], and radiative relaxation happens on a short time scale (lifetime ~1 fs), the excited-state asymmetry is preserved in the decay process because the molecules do not have time to rotate. Similarly, the molecular KL data in Fig. 2 represent linear dichroism as a function of the angle between the incident and emitted polarizations, $\vec{e}_1$ and $\vec{e}_2$, due to anisotropy in the resonant absorption process. (We note angular dependences of SO ratios have been known in surface science for some time and interpreted in terms of surface structure and scattering [17,18].)

To understand the non-atomic-like behavior exhibited in Fig. 2, and to allow a more complete analysis of the data, detailed relativistic calculations, including SO coupling, were performed. For KL decay, the final state has a hole in the $2p_{1/2}$ or $2p_{3/2}$ level, and the spectral and polarization properties of RIXS are guided by the transition matrix element [19],

$$F^{\alpha\beta}_{2p_\gamma \mathrm{val}^*} = \sum_c \frac{\langle 2p_\gamma^{-1}\mathrm{val}^{*+1}|\mathcal{D}_\alpha|1s^{-1}\mathrm{val}^{*+1}\rangle\langle 1s^{-1}\mathrm{val}^{*+1}|\mathcal{D}_\beta|0\rangle}{(\omega_1 - \omega_{\mathrm{cf}}) + i\Gamma_c/2}, \quad (1)$$

where $|0\rangle$ is the initial (ground) state, $2p_\gamma^{-1}$ is the final state with a hole in one of the three $2p_{x,y,z}$ orbitals ($2p_z$ lies along the symmetry axis), γ represents the SO sublevels, α and β represent the x, y, z components of the dipole operator $\mathcal{D}$, and the frequencies (polarization vectors) of the incident and emitted photons are ω_1 ($\vec{e}_1$) and ω_2 ($\vec{e}_2$), respectively. The lifetime broadening of the $1s^{-1}\mathrm{val}^{*+1}$ neutral core-excited state is Γ_c, and $\hbar\omega_{\mathrm{cf}}$ is the transition energy between this state and the final state γ. Because of SO coupling, the $2p_\gamma^{-1}\mathrm{val}^{*+1}$ final states are linear combinations of triplet and singlet nonrelativistic components.

Because the symmetry of the initial state is $^1\Sigma^+$ for HCl ($C_{\infty v}$) and $^1A_1$ for CF_3Cl (C_{3v}), $\langle 1s^{-1}\mathrm{val}^{*+1}|\mathcal{D}_\beta|0\rangle$ vanishes for $\beta = x, y$. Furthermore, if the final state has a core hole in $2pz$, the $\langle 2p_z^{-1}\mathrm{val}^{*+1}|\mathcal{D}_{x,y}|1s^{-1}\mathrm{val}^{*+1}\rangle$ terms vanish. If the final state has a core hole in $2p_{xy}$, only the terms $\langle 2p_{x,y}^{-1}\mathrm{val}^{*+1}|\mathcal{D}_{x,y}|1s^{-1}\mathrm{val}^{*+1}\rangle$ do not vanish. For randomly oriented molecules, one has to perform an average over all spatial orientations [20], leading to a mean-squared amplitude given by

$$\langle |F_{2p_\gamma \mathrm{val}^*}|^2\rangle = 2(1 + 2\cos^2\theta)[F^{zz}_{2p_z\mathrm{val}^*}F^{zz*}_{2p_z\mathrm{val}^*}]W^z_{\gamma,S} + 4(2 - \cos^2\theta)[F^{xz}_{2p_x\mathrm{val}^*}F^{xz*}_{2p_x\mathrm{val}^*}]W^x_{\gamma,S}, \quad (2)$$

where θ is the angle between $\vec{e}_1$ and $\vec{e}_2$. We introduce $W^z_{\gamma,S}$ and $W^{x,y}_{\gamma,S}$ as the nonrelativistic triplet and singlet $2p_z^{-1}\mathrm{val}^{*+1}$ and degenerate $2p_{x,y}^{-1}\mathrm{val}^{*+1}$ populations in the $2p_\gamma^{-1}\mathrm{val}^{*+1}$ relativistic configuration. This formula explicitly includes polarization dependencies for the $2p_{x,y}$ and $2p_z$ components. The $2p \rightarrow 1s$ oscillator strength is given by the transition probability between the localized Cl $1s$ and the nonrelativistic singlet $^1A_1(^1\Sigma^+)$ or degenerate $^1E(^1\Pi)$ $2p$ components, multiplied by the weights (populations) of these states in the relativistic configuration.

The ground-state potential-energy surface (PES) along the C-Cl bond in CF_3Cl is represented by a Morse potential with parameters given by Hahndorf *et al.* [21], yielding vibrational frequencies (470 cm^{-1}) close to experiment (476 cm^{-1}). For HCl, we used the PES described in [6]. The SO interaction, including the full Breit-Pauli coupling [22–24] integral package in GAMESS(US) [25], was used for calculations of $2p^{-1}$ core-excited states. Spin-orbit-coupling calculations were performed on variational CI wave functions, dubbed SO-CI [26]. The CI active space includes the three occupied $2p_{x,y,z}$ inner shells and the 80 lowest unoccupied virtual orbitals, all derived from the nonrelativistic $2s^{-1}\mathrm{val}^*$ potential. The core-excited reference wave function was represented by a generalized $2s^{-1}\mathrm{val}^*$ singlet state to avoid orientational effects artificially induced in the calculations using $2p_{x,y,z}^{-1}\mathrm{val}^*$ states. Because the $2s$ and $2p$ orbitals are close in energy ($\Delta E \sim 70$ eV [27]), equivalent relaxation effects are expected. The low-lying $2p^{-1}\mathrm{val}^*$ SO components, including nonrelativistic states for CF_3Cl and HCl at the equilibrium bond lengths (1.75 and 1.28 Å, respectively), were calculated *ab initio*. The calculated SO splitting of the Cl $2p$ orbitals is ≈ 1.65 eV for both molecules, as observed experimentally. If the nonrelativistic states of the final-state configurations did not differ in energy, the sublevels would collapse into two atomiclike Cl $2p^{-1}$ SO components, with an intensity ratio between them of exactly 2:1. This is the case at large interatomic distances, where MF and STE effects are weak, but it is not the case at the shorter distances in a bound molecule. Thus, the nonrelativistic states $^1\Sigma^+(^1A_1)$ and $^1\Pi(^1E)$ in HCl (CF_3Cl) are nondegenerate.

Performing further analysis of the KL-emission spectra using information gleaned from the calculations, it is possible to estimate the $2p_\gamma^{-1}\mathrm{val}^{*+1}$ contributions to the (nominal) $2p_{1/2}$ and $2p_{3/2}$ molecular SO peaks. First, theory indicates only the three nonrelativistic singlet $2p_{x,y,z}^{-1}$ subcomponents are nonvanishing, and two of them, $2p_x^{-1}$ and $2p_y^{-1}$, are degenerate. Thus, it is sufficient to fit the $2p_{1/2}$ and $2p_{3/2}$ SO peaks with two subcomponents each, for a total of four per spectrum. For better results, four-component fits were performed simultaneously for the spectra taken at all ten polarization angles. The profiles (shapes and widths) used to represent the four components were obtained from theory [Eq. (1)] based on the reasonable assumption (needs a reference) the potentials of the $1s^{-1}\mathrm{val}^{*+1}$ and $2p_\gamma^{-1}\mathrm{val}^{*+1}$ states are parallel. This assumption naturally yields the same energy widths for all four components, and this width was fixed in the fitting procedure. In contrast, relative intensities and energy positions of the four components were varied in the multispectra fits, with the former (intensities) being the results of primary interest.

Figure 3 shows spectra obtained at 0° and 90° fit with four components. Energy splittings between the $2p_z$ and $2p_{x,y}$ components obtained from the fits were 0.14 eV for HCl and 0.17 eV for CF_3Cl, in reasonable agreement with theory. However, the results were fairly insensitive to these values; variation of the splittings by up to ± 0.1 eV achieved the same fit quality. In contrast, the fits were sensitive to small variations in the relative intensities of the $2p_z$ and $2p_{x,y}$ contributions to the $2p_{3/2}$ and $2p_{1/2}$ SO components; changes of only $\pm 1\%$ markedly degrade the fits. For HCl, we find $2p_z$ contributes 54% to $2p_{3/2}$ and 46% to $2p_{1/2}$ ($2p_{x,y}$ contributes 59% and 41%, respectively). Similarly, in CF_3Cl, we find $2p_z$ contributes 46% to $2p_{3/2}$ and 54% to $2p_{1/2}$. These experimentally derived

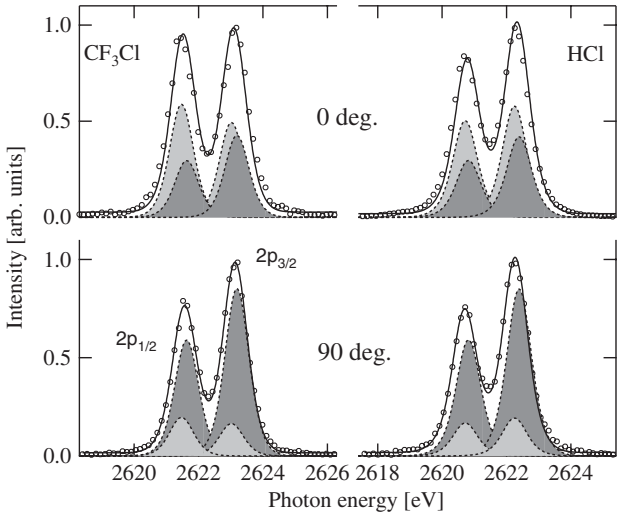

FIG. 3. Experimental *KL* emission spectra (circles) obtained at 0° and 90° between the incident and emitted x-ray polarization vectors for HCl and CF_3Cl. Solid curves are fits to the spectra. For each spin-orbit component, two nondegenerate sublevels, $2p_z(^1A_1)$ (light gray) and $2p_{xy}(^1E)$ (dark gray), are included.

populations agree well with our calculated results for $2p_z$: 51% and 49% in HCl, and 46.5% and 53.5% in CF_3Cl, respectively. These results, which differ by molecule, indicate the make-up of each SO component is dependent on chemical environment, including interatomic distance, which influences mixing of triplet and singlet states caused by the SO interaction.

In conclusion, polarized-RIXS measurements of HCl and CF_3Cl following resonant excitation of a 1*s* core electron to the first unoccupied molecular orbital were compared to theoretical calculations accounting for SO coupling. The technique is demonstrated to be sensitive to subtle changes in the SO interaction due to MF and STE effects; polarized RIXS thus offers a unique opportunity to determine spin-orbit-component populations, providing a new probe of MF effects on electronic structure. Finally, this technique, complementary to electron spectroscopy because it probes neutral molecular states, should be generally applicable to any molecular system.

The authors thank the staff of the ALS for their support. The UNLV team was funded by NSF under Grant No. PHY-05-55699. Financial support of PICS by CNRS is gratefully acknowledged. Computations were performed at the Institut du Développement et des Ressources en Informatique Scientifique (IDRIS), France.

[1] M. Kivilompolo *et al.*, J. Phys. B **33**, L157 (2000).
[2] K. Ellingsen *et al.*, Phys. Rev. A **55**, 2743 (1997).
[3] E. Kukk *et al.*, J. Phys. B **33**, L51 (2000).
[4] G. Turri *et al.*, Phys. Rev. Lett. **92**, 013001 (2004).
[5] R. Fink, M. Kivilompolo, and H. Aksela, J. Chem. Phys. **111**, 10 034 (1999).
[6] M. Simon *et al.*, Phys. Rev. A **73**, 020706 (2006).
[7] M. Žitnik *et al.*, Phys. Rev. A **76**, 032506 (2007).
[8] P. A. Raboud *et al.*, Phys. Rev. A **65**, 062503 (2002).
[9] S. Carniato *et al.*, Chem. Phys. Lett. **439**, 402 (2007).
[10] F. Gel'mukhanov *et al.*, Phys. Rev. A **59**, 380 (1999).
[11] F. Gel'mukhanov and H. Ågren, Phys. Rep. **312**, 87 (1999).
[12] R. C. C. Perera, G. Jones, and D. W. Lindle, Rev. Sci. Instrum. **66**, 1745 (1995).
[13] A. C. Hudson *et al.*, Rev. Sci. Instrum. **78**, 053101 (2007).
[14] D. W. Lindle *et al.*, Phys. Rev. Lett. **60**, 1010 (1988).
[15] D. W. Lindle *et al.*, Phys. Rev. A **43**, 2353 (1991).
[16] Nondipole effects in RIXS at the Cl *K* edge can be ignored for molecules with a single chlorine atom. See J. D. Mills *et al.*, Phys. Rev. Lett. **79**, 383 (1997).
[17] E. L. Bullock *et al.*, Surf. Sci. **352**, 352 (1996).
[18] H. W. Yeom *et al.*, Surf. Sci. **395**, L236 (1998).
[19] J. J. Sakurai, in *Advanced Quantum Mechanics* (Addison-Wesley Reading, MA, 1967).
[20] Y. Luo, H. Ågren, and F. Gel'mukhanov, J. Phys. B **27**, 4169 (1994).
[21] I. Hahndorf *et al.*, Chem. Phys. Lett. **231**, 460 (1994).
[22] T. R. Furlani and H. F. King, J. Chem. Phys. **82**, 5577 (1985).
[23] H. F. King and T. R. Furlani, J. Comput. Chem. **9**, 771 (1988).
[24] D. G. Fedorov and M. S. Gordon, J. Chem. Phys. **112**, 5611 (2000).
[25] M. W. Schmidt *et al.*, J. Comput. Chem. **14**, 1347 (1993).
[26] We also performed calculations based on 2nd order perturbation theory using the MCQDPT Multi-reference perturbation theory, which will be discussed in a future publication.
[27] D. Céolin *et al.*, J. Chem. Phys. **126**, 084309 (2007).